JOURNAL OF SCIENCE, TECHNOLOGY AND ENGINEERING RESEARCH
Bilim, Teknoloji ve Mühendislik Araştırmaları Dergisi, (2023) - 4(2): 78-89
ISSN : 2717-8404 *https://dergipark.org.tr/en/pub/jster*

RESEARCH ARTICLE

Medical Image Enhancement Based on Volumetric Tissue Segmentation Fusion (Uni-Stable-3D Method)

* Ihab ELAFF

* Department of Computer Engineering, Faculty of Engineering and Natural Sciences, Uskudar University, Istanbul, Turkey
email: ihab.elaff@uskudar.edu.tr

HIGHLIGHTS

- *The Uni-Stable-3D is a new method for 3D medical image enhancement.*
- *The Uni-Stable-3D image is almost universal as it combines variety of algorithms points of views into one 3D probability map*
- *Uni-Stable-3D Images reduces boundary-overlapping among different tissues.*

Keywords:

- Uni-Stable
- WM
- GM
- CSF
- Brain Segmentation
-

Article Info:

Received : 11 February 2023
Accepted : 6 June 2023

DOI:
10.53525/jster.1250050

***Correspondence:**
Ihab ELAFF
ihab.elaff@uskudar.edu.tr
Phone : +90 534 3617233

GRAPHICAL ABSTRACT

The Uni-Stable-3D is a new method for 3D medical image enhancement which produces 3D Images of high contrast from the scanned anisotropic scaling images.

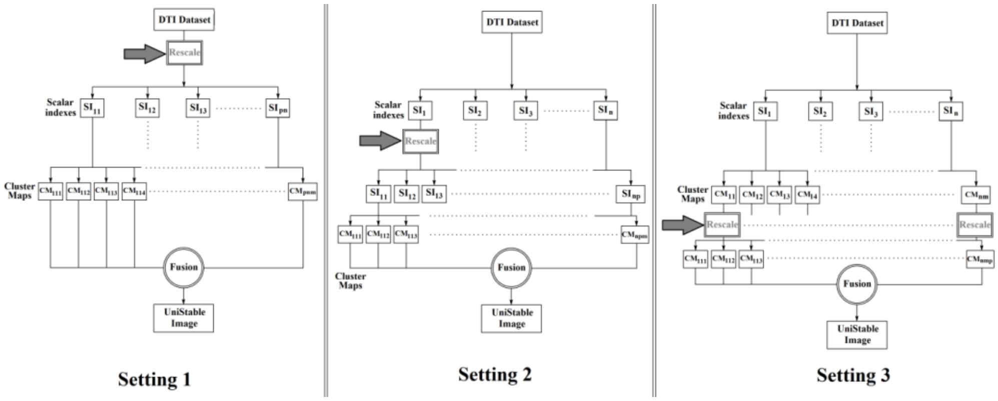

Figure Different settings of Uni-Stable-3D method

Aim of Article: *Medical image enhancement based on 3D reconfiguring of anisotropic images scans to produce images of high contrast which are suitable for segmentation using any clustering algorithm.*

Theory and Methodology: *This is done by estimating some intermediate slices through resizing the original DTI scans. Rescaling has been achieved at three different levels: rescaling of eigenvalues of diffusion, rescaling the Scalar Indexes from the original eigenvalues, and rescaling the cluster maps of the segmentation of the original Scalar Indexes. Four interpolation methods have been employed at each level and four clustering algorithms have been employed in the process.*

Findings and Results: *Univeral and stable 3D medical images with high contrats.*

Conclusion : *The Uni-Stable-3D images are almost universal as they combine a variety of algorithms points-of-views into one 3D probability map. This reduces boundary-overlapping among different tissues, and hence improves the uniqueness of the segmentation problem solution.*

JOURNAL OF SCIENCE, TECHNOLOGY AND ENGINEERING RESEARCH
Bilim, Teknoloji ve Mühendislik Araştırmaları Dergisi, (2023) - 4(2): 78-89
ISSN : 2717-8404 https://dergipark.org.tr/en/pub/jster

RESEARCH ARTICLE

Medical Image Enhancement Based on Volumetric Tissue Segmentation Fusion (Uni-Stable-3D Method)

* Ihab ELAFF

* Department of Computer Engineering, Faculty of Engineering and Natural Sciences, Uskudar University, Istanbul, Turkey
email: ihab.elaff@uskudar.edu.tr

Citation:

Elaff, I. (2023). *Medical image enhancement based on volumetric tissue segmentation fusion (Uni-Stable 3D method),* Journal of Science Technology and Engineering Research, 4(2): 78-89. DOI: 10.53525/jster.1250050

HIGHLIGHTS

- *Novel technique for 3D medical image enhancement that is titled as: Uni-Stable-3D Images.*
- *The Uni-Stable-3D image is almost universal as it combines variety of algorithms points of views into one 3D probability map*
- *Uni-Stable-3D Images reduces boundary-overlapping among different tissues*

Article Info

Received : 11February 2023
Accepted : 06 June 2023

DOI:
10.53525/jster.1250050

***Corresponding Author:**
Ihab ELAFF
ihab.elaff@uskudar.edu.tr
Phone: +90 123 4567890

ABSTRACT

The Uni-Stable-3D is a new method for 3D medical image enhancement which produces 3D Images of high contrast from the DTI anisotropic images. This is done by estimating some intermediate slices through resizing the original scans. Rescaling has been achieved at three different levels: rescaling of eigenvalues of diffusion, rescaling the Scalar Indexes from the original eigenvalues, and rescaling the cluster maps of the segmentation of the original Scalar Indexes. Four interpolation methods have been employed at each level and four clustering algorithms have been employed in the process. The Uni-Stable-3D produces images which are almost universal as the method combines a variety of algorithms points-of-views into one 3D probability map. This reduces boundary-overlapping among different tissues, and hence improves the uniqueness of the segmentation problem solution. The stability factor of the Uni-Stable-3D images has been measured using maximum match analysis between the cluster maps which are generated from Uni-Stable-3D images by a variety of clustering methods with respect to true fact references for 5 different brains. The resultant standard deviations of Uni-Stable-3D images maximum match analysis in both threshold and tissue to brain ratio are much lower than Mean Diffusivity and Fractional Anisotropy scalar indexes for both CSF/non-CSF and WM/non-WM respectively.

Keywords: *Uni-Stable, WM, GM, CSF, Brain Segmentation*

I. INTRODUCTION

Computer-aided diagnosis (CAD) is considered one of the major research subjects in medical imaging and diagnostic radiology [1, 2]. With CAD, radiologists use the computer output as a "second opinion" and make the final decisions. The ability to produce high contrast medical images has its importance in diagnosing, evaluation and computer-based simulation of a certain tissue or organ.

Medical imaging such as CT-scan and MRI are usually accomplished in an anisotropic manner where the planer resolution spacing and slice to slice spacing are (usually) different [3]. This makes the 2D based segmentation process of scans not able to provide the accurate 3D bounds of the tissues, where this shows the necessity for estimating some intermediate plans to solve that problem. The estimation of some intermediate plans requires 3D image resizing to be involved in the process.

In addition to the anisotropic spacing problem, the macroscale resolution of scanners [4, 5] causes boundary-overlapping between neighbor tissues in medical images [6 – 8]. With those 2 problems, the estimation of an accurate 3D tissue's boundary becomes in demand.

When only 2D images of the original scans are employed for processing tissue in 3D, it would act like resizing this image using the nearest interpolation method. However, by applying other interpolation methods such as Linear, Cubic, Lanczos2 or Lanczos3 [9, 10], more accurate estimation for the intermediate plans would be expected. Linear interpolation estimates intermediate states over a tangent line between two measured states, while Cubic uses Gaussian smoothing curve and Lanczos methods depend on the Sinc function.

The most important image segmentation techniques are: threshold based methods, clustering based methods, edge based methods, region based methods, watershed based methods, Partial Differential Equation (PDE) based methods and Artificial Neural Network (ANN) based methods [11]. Clustering base methods such as Otsu algorithm [12], K-Means algorithm [13], Expectation Maximization (EM) algorithm [14], C-Means algorithm, Fuzzy C-Means (FCM) algorithm and Spatial constrained Fuzzy C-Means (SFCM) algorithm [15], Markov Random Field (MRF) algorithm and Iterated Conditional Modes (ICM) algorithm [16] are widely used with medical images.

It was reported that there is no unique solution to the segmentation problem, because of the effect of the used imaging modality on the segmentation process; different results are obtained by changing clustering method and/or the selected numbers of clusters [5, 7, 8, 15, 16]. Many models have been represented for 3D brain segmentation. Duy M. H. Nguyen et. al. produces a 3D brain tissue segmentation using Gaussian Mixture Models (GMMs), Convolution Neural Networks (CNNs) and Deep Neural Networks (DNNs)[17]. Yuankai Huo et.al. proposed the Spatially Localized Atlas Network Tiles (SLANT) method to distribute multiple independent 3D Fully Convolutional Networks (FCN) for high-resolution whole brain segmentation[18]. Fareeen Ramzan et.al. employ a network for the segmentation of multiple brain regions has been proposed that is based on 3D convolutional neural networks and utilizes residual learning and dilated convolution operations to efficiently learn the end-to-end mapping from MRI volumes to the voxel-level brain segments[19]. Youyong Kong et.al. presents a novel algorithm for brain tissue segmentation based on supervoxel and graph filter. Firstly, an effective supervoxel method is employed to generate effective supervoxels for the 3D MRI image. Secondly, supervoxels are classified into different types of tissues based on filtering of graph signals [20]. Kamarujjaman represents a novel 3D unsupervised spatial fuzzy-based brain MRI volume segmentation technique in the presence of intensity inhomogeneity and noise. Instead of static masking, dynamic 3D masking has been proposed to measure the correlation among neighbors [21]. Results from stated methods targeting either high resolution scans or depend on one segmentation technique. According to our best knowledge, the present 3D segmentation methods don't consider the lost information in the spacing between slices, which in turn produce approximate results for volumetric shapes.

One solution in a former research [22] that has been developed to produce Uni-Stable images where segmentation results are relatively stable regardless of the use of the clustering method. The maximum match analysis of 5 brains for CSFUni and WMUni gives values 0.29±0.002 and 0.39±0.003 respectively. However, the Uni-Stable method, also, did not consider the spacing between slices. This research represents an improvement to the Uni-Stable method by re-producing medical image slices in a way to cover spaces between scanned slices using combinations of interpolation methods and cluster maps. This will re-generate volumetric 3D images which are universal and stable for the segmentation process using any algorithm and produce fewer overlapping errors.

II. MATERIALS AND METHODS

A. Dataset

Datasets of this study have been obtained from John Hopkins Medical Institute website. These datasets consist of brains' DTI volume data where each brain is scanned in 50 slices with a resolution of 256 × 256 voxels per slice. In every slice, the voxel width and height are 0.9375 mm and the spacing between each successive slice is 2.5mm. Some scalar Indices (SI) for those DTI images have been generated, namely: Mean Diffusivity (MD), Fractional Anisotropy (FA), Rational Anisotropy (RA), Matisuia Anisotropy (MA), Linear Anisotropy (Cl), Spherical Anisotropy (Cs) , Volume Ratio (VR), Angular Anisotropy (AA), and Diffusion

Volume (DV) [4, 5, 6, 23 - 27].

B. Uni-Stable-3D Images

The lack of solution uniqueness in the medical image segmentation problem is because of different medical imaging types, the selected clustering algorithm, and interpolation method of rescaling its order where each setting has its own estimate. A new approach for 3D brain image segmentation based on interpolating anisotropic brain scans from Diffusion Tensor Imaging modality. As axial brain scans are usually accomplished in anisotropic spacing where the plane resolution spacing and slice to slice spacing are usually different, then 2D-based segmentation of brain tissues cannot provide accurate 3D bounds of the tissues. This is where 3D image interpolation should be involved in the process. The main concerns of the accurate 3D brain tissues are the suitable stage order of the interpolation in the process, the suitable interpolation methods and the suitable Scalar indexes for that job.

The Uni-Stable method [17] was originally developed for generating high contrast 2D images based on DTI scans, where the Uni-Stable method has been proved to be universal where many segmentation settings are considered, and their segmentation results are relatively independent of the applied clustering method, which makes it relatively stable. The process starts by producing different SI from eigenvalues of the DTI data, generating Cluster Maps (CM) from the generated SIs and finally fusing the generated CMs into one probability map, which is the Uni-Stable Image, where this process makes sure that common points will have more probability than less common points.

In the way to upgrade this method to a 3D version, a resizing stage would be added to estimate some intermediate slices between originally scanned ones, which in turn will solve the anisotropic spacing problem. The selected interpolation method of the resize operation and its order in the process plays a basic role that affects the Uni-Stable-3D image generation as shown in Figure 1. The first setting (Setting 1) is resizing the eigenvalues of the DTI images before the other stages. The 2nd (Setting 2) is to generate SI's from the original eigenvalues and then resize the SI maps. The last one (Setting 3) is to generate the CM's from the original SIs and then resize them before the fusion process. Four interpolation methods are tested for 3D image resizing: Linear, Cubic, Lanczos2 and Lanczos3. For N SIs, which contain clear features about the required tissues; M clustering methods with P different Interpolation methods generate N × M × P estimates of normalized CMs. Normalized Uni-Stable-Image IMGUni is generated by fusing these CMs together, where:

$$\mathrm{IMG}_{\mathrm{Uni.}} = \frac{\sum_{n=1}^{N}\sum_{m=1}^{M}\sum_{p=1}^{P} CM_{nmp}}{Max(\sum_{n=1}^{N}\sum_{m=1}^{M}\sum_{p=1}^{P} CM_{nmp})} \;\ldots\ldots\ldots\ldots (1)$$

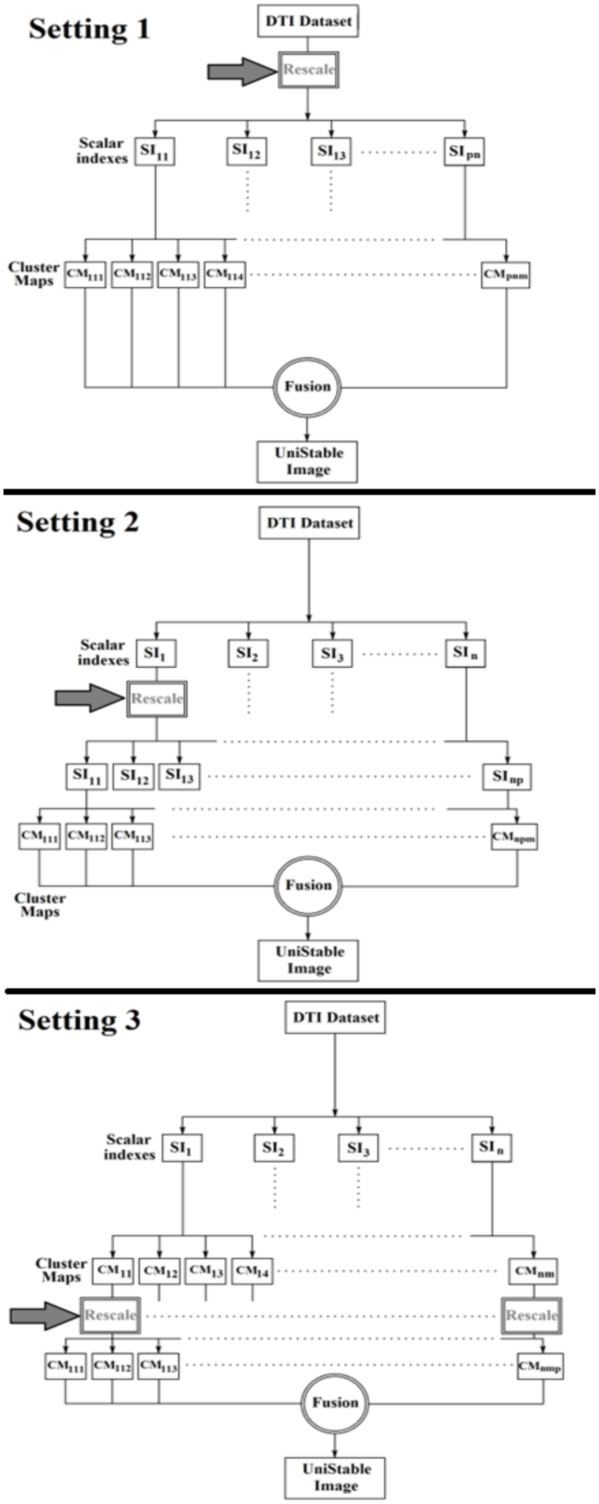

Figure 1 Different settings of Uni-Stable-3D method

In this study, brain data has been resized from 256x256x50 to 256x256x200 using three different settings to estimate some intermediate slices between originally scanned ones.

C. CSF/non-CSF 3D Uni-Stable-Image generation

For generating CSF/non-CFS 3D-Uni-Stable-Images (CSFUni), some SI's are used, namely: MD, DV, λ1, λ2, and λ3. Those SI has been clustered using 4 different clustering algorithms, namely: Otsu, KM, FCM and SFCM. Rescaling using four interpolation methods has been tested in the process with the different location. For each setting, 80 different cluster maps are produced. Cluster maps are then fused into one image as shown in Figure 2.

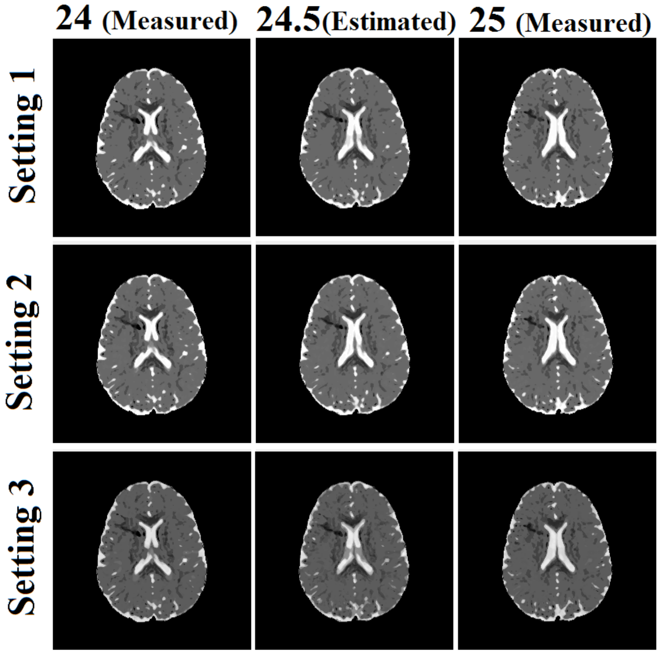

Figure 2 CSF/non-CSF Uni-Stable-3D images using different settings for 2 measured slices and one estimated slice in the middle.

Table 1. Different Settings for CSF/non-CSF Uni-Stable-3D Image Generation**.**

	Rescale Level	**Interpolation Methods**	**Clustering Methods**	**Scalar Indexes**	**Number of Fused Cluster Maps**
Setting 1	Eigenvalues Rescale	Linear, Cubic, Lanczos2, Lanczos3	Otsu, K-Means, FCM, SFCM	MD, DV, λ_1, λ_2, λ_3	80
Setting 2	Scalar Indexes Rescale	Linear, Cubic, Lanczos2, Lanczos3	Otsu, K-Means, FCM, SFCM	MD, DV, λ_1, λ_2, λ_3	80
Setting 3	Cluster Maps Rescale	Linear, Cubic, Lanczos2, Lanczos3	Otsu, K-Means, FCM, SFCM	MD, DV, λ_1, λ_2, λ_3	80

D. WM/non-WM 3D Uni-Stable-Image generation

For generating WM/non-WM 3D-Uni-Stable-Images (WMUni), some SI's are used, namely: FA, RA, AA, MA, and Cl. Those SI has been clustered using 4 different clustering algorithms, namely: Otsu, KM, FCM and SFCM. Rescaling using four interpolation methods has been tested in the process with the different location. For setting 1, 40 different cluster maps are produced because only two interpolation methods re used and 80 different cluster maps are use in other settings. More justification would be indicated in the discussion and conclusion part about that. Finally, cluster maps are then fused into one image as shown in Figure 3.

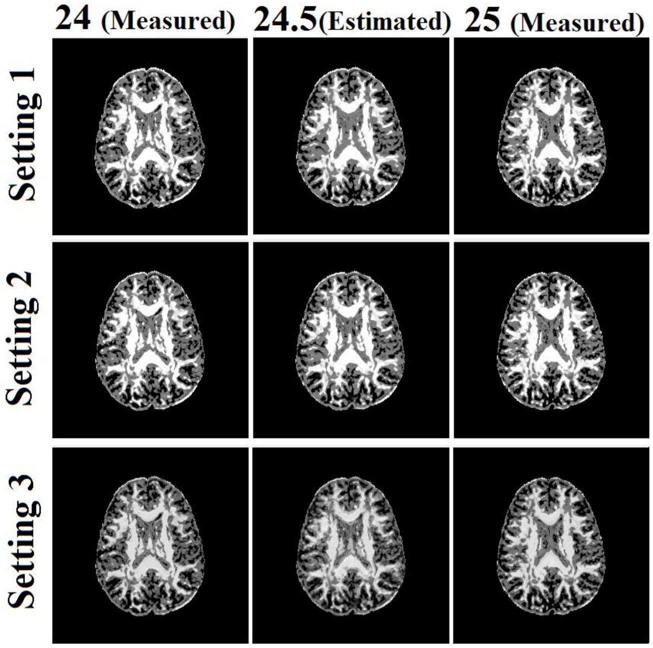

Figure 3 WM/non-WM Uni-Stable-3D images using different settings for 2 measured slices and one estimated slice in the middle.

Table 2. Different Settings for WM/non-WM Uni-Stable-3D Image Generation

	Rescale Level	**Interpolation Methods**	**Clustering Methods**	**Scalar Indexes**	**Number of Fused Cluster Maps**
Setting 1	Eigenvalues Rescale	Linear Cubic	Otsu, K-Means, FCM, SFCM	FA, RA, AA, MA, Cl	40
Setting 2	Scalar Indexes Rescale	Linear Cubic, Lanczos2, Lanczos3	Otsu, K-Means, FCM, SFCM	FA, RA, AA, MA, Cl	80
Setting 3	Cluster Maps Rescale	Linear Cubic, Lanczos2,	Otsu, K-Means, FCM,	FA, RA, AA,	80

		Lanczos3	SFCM	MA, Cl	

III. RESULTS

A. Reference Model

The usual SIs which are used in the brain image segmentation are FA and MD. For normalized MD images, a threshold with values around 0.3 can efficiently separate CSF/non-CSF [28] and for normalized FA images, a threshold with values between 0.25 and 0.45 can separate WM/non-WM [29]. As the original scans reflect the solid facts about the scans, so they should be taken as a comparison reference. For size consistency, the nearest interpolation is applied to resize the original FA and MD.

B. Non-Uni-Stable 3D images Segmentation

For the regular process, FA and MD are resized using linear interpolation or cubic interpolation after being calculated from the original eigenvalues [30]. However, more settings have been explored where FA and MD are resized according to the following tables:

Table 3. Different Settings for MD rescaling.

	Rescale Level	**Interpolation Methods**
MD1.1	Eigenvalues Rescale	Linear
MD1.2	Eigenvalues Rescale	Cubic
MD2.1	Scalar Indexes Rescale	Linear
MD2.2	Scalar Indexes Rescale	Cubic

Table 4. Different Settings for FA rescaling.

	Rescale Level	**Interpolation Methods**
FA1.1	Eigenvalues Rescale	Linear
FA1.2	Eigenvalues Rescale	Cubic
FA2.1	Scalar Indexes Rescale	Linear
FA2.2	Scalar Indexes Rescale	Cubic

And the four mentioned clustering methods are also applied on those images with maximum match as shown in Figure 4 and Figure 5. It is noticed that each clustering method has different threshold point and this is the normal case where non unique solution is obtained.

Referring to Maximum-Match analysis for 5 brains, the average mean and the average standard deviation of the clustering algorithm and regular threshold method and the CSF to Brain and WM to Brain ratios are given in Tables 5 and Table 6

Table 5 Average Mean and Average standard deviation of 5 human brains for maximum match Threshold value and CSF to Brain ratio based on MD Images of different settings

	Threshold	**CSF to Brain Ratio**
MD1.1	0.306±0.0118	18.75±1.07
MD1.2	0.306±0.0125	18.64±1.06
MD2.1	0.306±0.0118	18.75±1.07
MD2.2	0.306±0.0125	18.64±1.06

Table 6 Average Mean and Average standard deviation of 5 human brains for maximum match Threshold value and WM to Brain ratio based on FA Images of different settings

	Threshold	**WM to Brain Ratio**
FA1.1	0.371±0.0127	29.15±1.80
FA1.2	0.375±0.0142	28.57±1.92
FA2.1	0.355±0.0203	32.71±8.58
FA2.2	0.368±0.0109	28.26±1.56

C. 3 Uni-Stable 3D images Segmentation

Maximum-Match analysis for 5 brains is repeated again for 3D Universal images under the 3 settings (Figure 6, Figure 7, Table 7 and Table 8). In both Figure 6 and Figure 7: Otsu, K-Means and FCM curves are overlapping. The SFCM is shifted a little bit downward below them; however, all of them are aligned almost to the same threshold point. This indicates that segmentation results are almost independent from the clustering algorithm.

Quantitatively, the average mean and average standard deviation of 5 human brains for maximum match the threshold value and CSF to brain ratio based on 3D Universal images of both CSF/non-CSF and WM/non-WM under the different three settings are demonstrated in Table 7 and Table 8 respectively. The average mean values are almost the same such as Table 5 and Table 6; however, the average standard-deviation values are much lower than in the MD and FA cases. This indicates that segmentation of the Uni-Stable-3D images is almost independent of the clustering method.

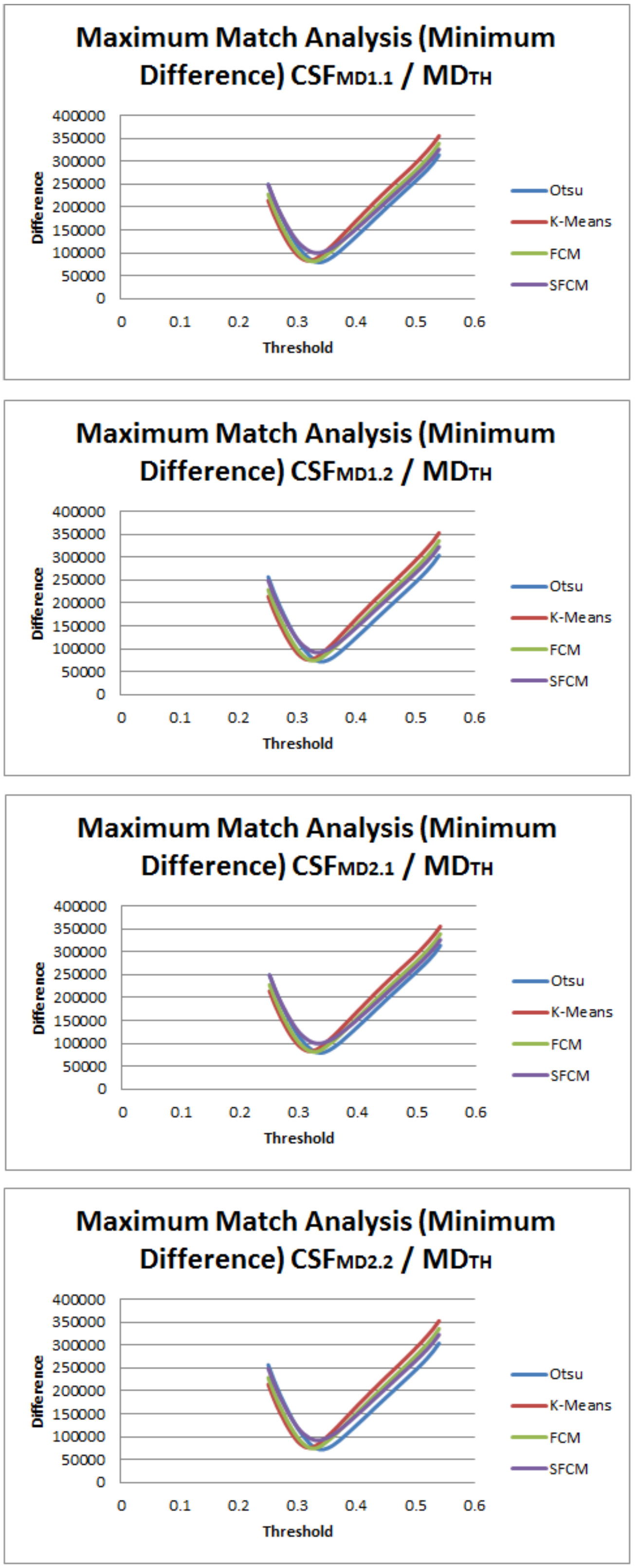

Maximum Match Analysis (Minimum Difference) $CSF_{MD1.1}$ / MD_{TH}

Maximum Match Analysis (Minimum Difference) $CSF_{MD1.2}$ / MD_{TH}

Maximum Match Analysis (Minimum Difference) $CSF_{MD2.1}$ / MD_{TH}

Maximum Match Analysis (Minimum Difference) $CSF_{MD2.2}$ / MD_{TH}

Figure 4 Maximum match analysis for CSF using MD Cluster Maps.

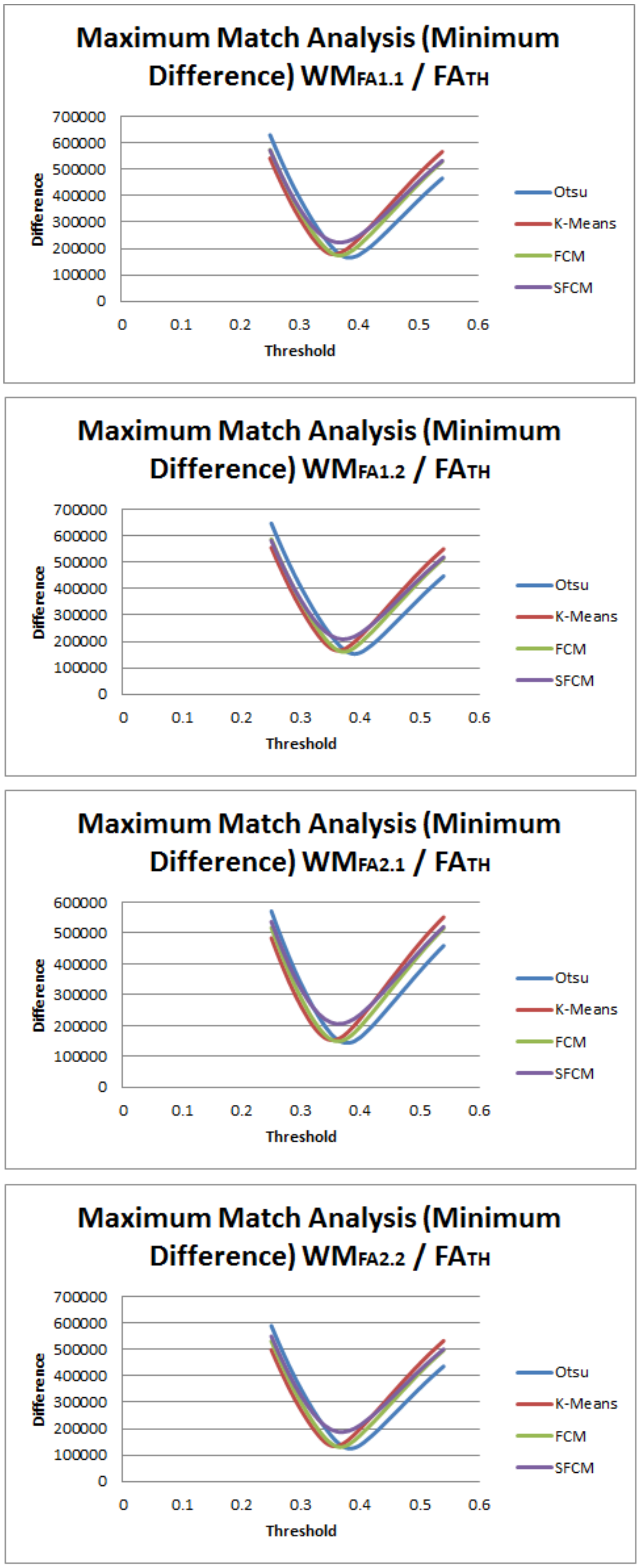

Maximum Match Analysis (Minimum Difference) $WM_{FA1.1}$ / FA_{TH}

Maximum Match Analysis (Minimum Difference) $WM_{FA1.2}$ / FA_{TH}

Maximum Match Analysis (Minimum Difference) $WM_{FA2.1}$ / FA_{TH}

Maximum Match Analysis (Minimum Difference) $WM_{FA2.2}$ / FA_{TH}

Figure 5 Maximum-Match analysis for WM using FA Cluster Maps.

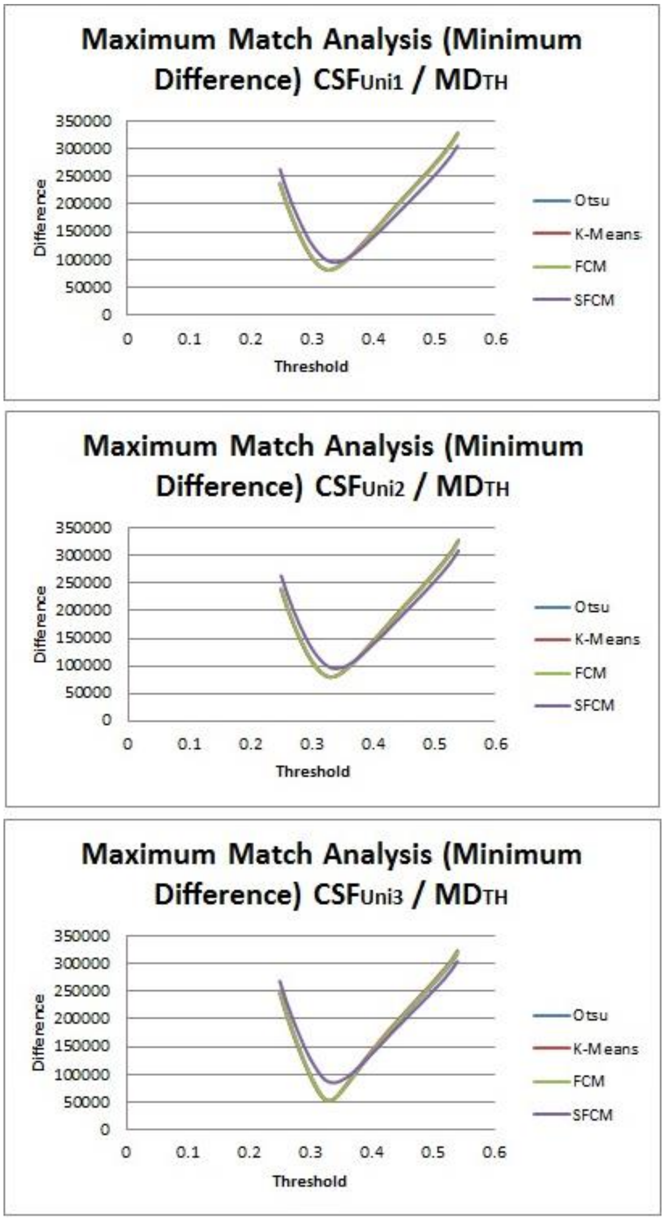

Figure 6 Maximum match analysis for CSF using CSF$_{Uni}$ Cluster Maps

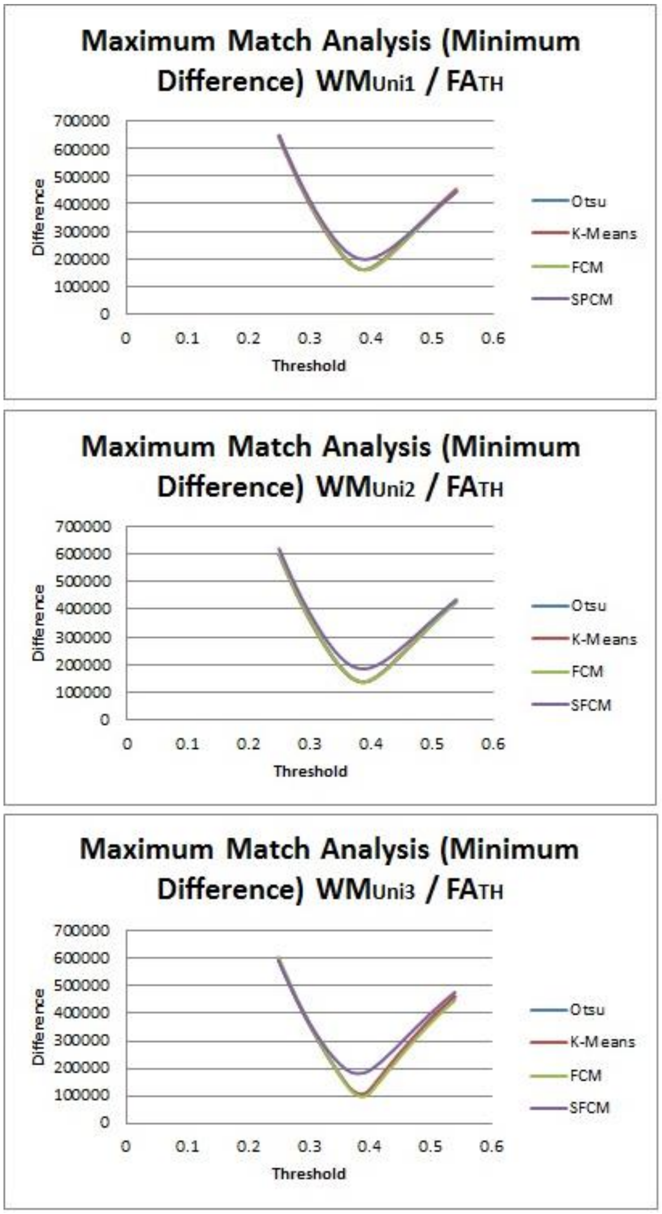

Figure 7 Maximum match analysis for WM using WM$_{Uni}$ Cluster Maps

Table 7 Average Mean and Average standard deviation of 5 human brains for maximum match Threshold value and CSF to Brain ratio based on 3D Universal CSF/non-CSF Images of different settings

		Threshold			**CSF to Brain Ratio**	
		AVG	STD		AVG	STD
CSF_{Uni1}	Brain1	0.3325	0.0050		17.80%	0.4570
	Brain2	0.2925	0.0050		17.82%	0.5550
	Brain3	0.3075	0.0050		18.99%	0.4440
	Brain4	0.3025	0.0050		21.59%	0.4890
	Brain5	0.3125	0.0050		16.01%	0.4200
	Average	0.310 ± 0.0050			18.44% ± 0.4730	
CSF_{Uni2}	Brain1	0.3325	0.0050		17.83%	0.3450
	Brain2	0.2925	0.0050		17.72%	0.4740
	Brain3	0.3075	0.0050		19.09%	0.4140
	Brain4	0.3025	0.0050		21.64%	0.4260
	Brain5	0.3125	0.0050		16.03%	0.3550
	Average	0.310 ± 0.0050			18.46% + 0.4028	
CSF_{Uni3}	Brain1	0.3325	0.0050		17.12%	0.2830
	Brain2	0.2925	0.0050		17.20%	0.4300
	Brain3	0.3025	0.0050		18.42%	0.3100
	Brain4	0.295	0.0058		21.13%	0.3790
	Brain5	0.3025	0.0050		16.10%	0.2740
	Average	0.305 ± 0.0052			17.99% ± 0.3352	

Table 8 Average Mean and Average standard deviation of 5 human brains for maximum match Threshold value and WM to Brain ratio based on 3D Universal WM/non-WM Images of different settings

		Threshold			**WM to Brain Ratio**	
		AVG	STD		AVG	STD
WM_{Uni1}	Brain1	0.39	0.0000		26.03%	0.3980
	Brain2	0.39	0.0000		28.41%	0.4230
	Brain3	0.39	0.0100		29.34%	0.8500
	Brain4	0.41	0.0050		25.31%	0.2360
	Brain5	0.36	0.0000		26.34%	0.5250
	Average	0.3865 ± 0.0030			27.085% ± 0.4864	
WM_{Uni2}	Brain1	0.39	0.0000		25.47%	0.3030
	Brain2	0.38	0.0000		27.80%	0.3550
	Brain3	0.38	0.0096		28.45%	0.7580
	Brain4	0.40	0.0000		24.81%	0.1660
	Brain5	0.36	0.0000		25.50%	0.3250
	Average	0.3825± 0.0019			26.4065% ± 0.3814	
WM_{Uni3}	Brain1	0.39	0.0050		26.14%	0.2620
	Brain2	0.39	0.0058		27.57%	0.2810
	Brain3	0.36	0.0350		33.39%	4.3550
	Brain4	0.40	0.0050		24.69%	0.2650
	Brain5	0.36	0.0000		25.46%	0.2100
	Average	0.38 ± 0.0102			27.4505% ± 1.0746	

For CSF/non-CSF Uni-Stable-3D images, Setting 3 provides the lowest average standard deviations and hence the most stable setup. For WM/non-WM Uni-Stable-3D images, Setting 2 provides the most stable setup.

IV. RESULT AND DISCUSSIONS

The Uni-Stable-3D is a new method for 3D medical image enhancement which produces images of high contrast from the scanned anisotropic images. It is basically an upgraded version of the former Uni-Stable method. This is done by estimating some intermediate slices by resizing the original scans. Rescaling has been achieved at three different levels: rescaling of eigenvalues of diffusion, rescaling the Scalar Indexes from the original eigenvalues, and rescaling the cluster maps of the segmentation of the original Scalar Indexes. Four different interpolation methods and four different clustering algorithms have been employed in the process.

The Uni-Stable-3D images are almost universal as they combine a variety of algorithms point-of-view into one 3D probability map. This reduces boundary-overlapping among different tissues, and hence improves the uniqueness of the segmentation problem solution.

The stability factor of the Uni-Stable-3D Images is measured by maximum match analysis between the cluster maps which are generated from Uni-Stable-3D images using a variety of clustering methods with respect to true fact references. For CSF/non-CSF, the true fact reference is taken as the threshold of MD scalar index's histogram after being resized using the nearest interpolation and again, for WM/non-WM, the true fact reference is taken as the threshold of FA scalar index's histogram after being resized using nearest interpolation. The same is repeated again but using cluster maps which are generated by applying some clustering methods to MD and FA.

The resultant standard deviations of Uni-Stable-3D images maximum match analysis in both threshold and tissue to brain ratio (tables 7 and 8) are much lower than MD and FA (tables 5 and 6). This reflects the stability of the Uni-Stable-3D images and indicates that they are almost clustering-algorithm-independent. The same process was repeated for 5 brains and the results were also the same.

Referring to the former research [22] that has been developed to produce Uni-Stable images based on multi-2D slices; for the same 5 brains, maximum match analysis for CSFUni and WMUni, there are no significant changes compared to Uni-Srable-3D method in mean values and SD values are still relatively very small in both cases (Table 9). Those minor differences are due to the interpolation process used in the Uni-Stable-3D with the advantage of covering the gaps between 2 successive slices.

Table 9 Comparison between clustering results of Uni-Stable method and Uni-Stable-3D method.

CSF/non–CSF		WM/non–WM	
CSF_{Uni}	0.29±0.002	WM_{Uni}	0.39±0.003
CSF_{Uni1}	0.310 ± 0.0050	WM_{Uni1}	0.3865 ± 0.0030
CSF_{Uni2}	0.310 ± 0.0050	WM_{Uni2}	0.3825± 0.0019
CSF_{Uni3}	0.305 ± 0.0052	WM_{Uni3}	0.38 ± 0.0102

Cubic, Lanczos2 and Lanczos 3 produce some negative values because of their kernel function, which can be eliminated. However, Lanczos2 and Lanczos3 Interpolation methods might not be suitable to be used in the level of resizing the eigenvalues because they depend on Sinc function. As the Sinc function oscillates, some small positive values could be produced in the background zone. Because of the rational nature of WM/non-WM scalar index calculations, extra regions would be generated in the background zone such as FA images (Figure 8). However, for integration based scalar indexes which are used to find CSF/non-CSF scalar indexes such as MD, these small values have almost no effect (Figure 8).

Finally, it is concluded that the Uni-Stable-3D method might be a straightforward solution for the segmentation problem of medical images, where the segmentation process can be achieved using only one Uni-Stable-3D image and any clustering method.

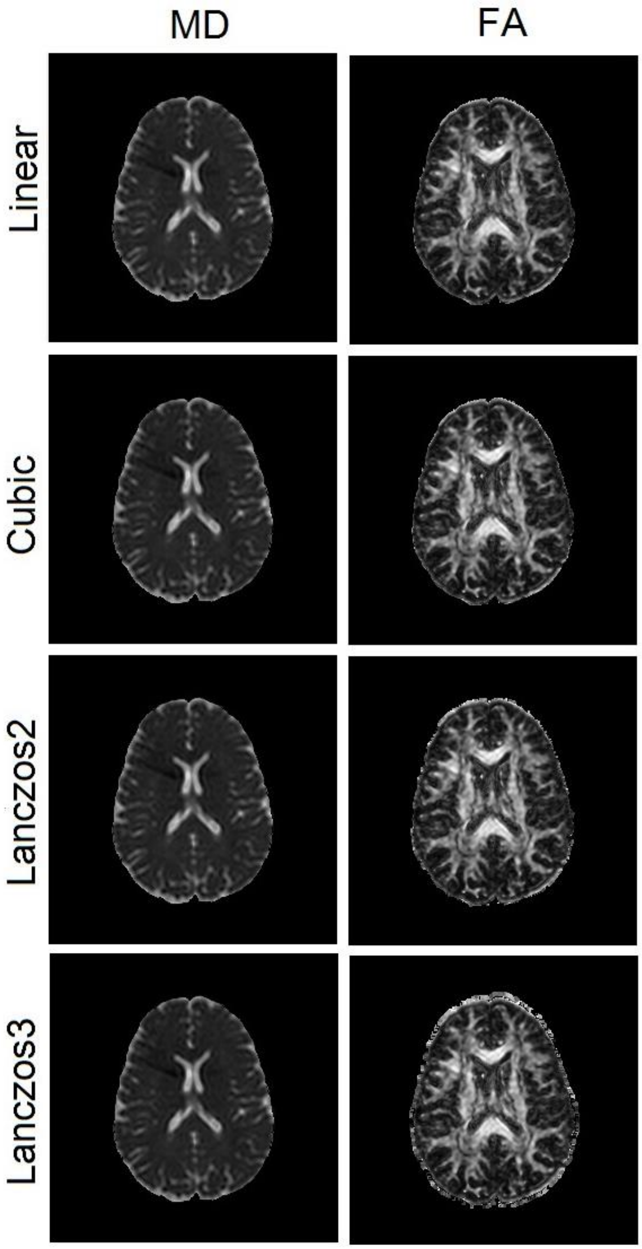

Figure 8 The Effect of some Interpolation methods for eigenvalues on the generated scalar indexes.

CONFLICTS OF INTEREST

They reported that there was no conflict of interest between the authors and their respective institutions.

RESEARCH AND PUBLICATION ETHICS

In the studies carried out within the scope of this article, the rules of research and publication ethics were followed.

ACKNOWLEDGMENT

Laboratory of Brain Anatomical MRI – Johns Hopkins Medical Institute at Johns Hopkins University for provision of DT-MRI data and DTI-Studio utility.

REFERENCES

[1] Doi K., Computer-aided diagnosis in medical imaging: Historical review, current status and future potential. Computerized Medical Imaging and Graphics. 2017; 31(4):198-211. DOI: 10.1016/j.compmedimag.2007.02.002

[2] Li Q, Nishikawa RM, editors. Computer-Aided Detection and Diagnosis in Medical Imaging. Taylor & Francis, CRC Press, New York; 2015.

[3] Neubert A, Salvado O, Acosta O, Bourgeat P, Fripp J. Constrained reverse diffusion for thick slice interpolation of 3D volumetric MRI images. Computerized Medical Imaging and Graphics 2012; 36(2): 130-138. DOI: 10.1016/j.compmedimag.2011.08.004.

[4] Mori S. Introduction to Diffusion Tensor Imaging.1st ed., Oxford, UK: Elsevier, 2007.

[5] Liu T, Li H, Wong K, Tarokh A, Guo L, Wong S. Brain Tissue Segmentation Based on DTI Data. Neuroimage 2007; 38: 114-23. DOI: 10.1016/j.neuroimage.2007.07.002

[6] Zarei M, Johansen Berg H, Matthews PM. Diffusion Tensor Imaging and Tractography in Clinical Neurosciences. Iran J Radiol 2003; 1: 45-52.

[7] Khotanlou H, Colliot O, Atif J, Bloch I. 3D Brain Tumor Segmentation in MRI Using Fuzzy Classification, Symmetry Analysis and Spatially Constrained Deformable Models. Fuzzy Set Syst 2009; 160: 1457-1473. DOI:10.1016/j.fss.2008.11.016

[8] Dubey RB,Hanmandlu M,Gupta SK,Gupta SK. The Brain MR Image Segmentation Techniques and use of Diagnostic Packages. Acad Radiol. 2010; 17: 658 – 671. DOI:10.1016/j.acra.2009.12.017

[9] Getreuer P. Linear Methods for Image Interpolation, Image Processing On Line, 2011; 1:238–259. DOI:10.5201/ipol.2011.g_lmii

[10] Glassner AS. Graphics Gems. 1st ed., Academic Press Inc., 1993.

[11] Dhal KG, Das A, Ray S, Galvez J, Das S. Nature Inspired Optimization Algorithms and Their Application in Multi Thresholding Image Segmentation. Archives of Computational Methods in Engineering (2020) 27:855–888. DOI: 10.1007/s11831-019-09334-y

[12] Otsu N. A threshold selection method from gray-level histograms. IEEE T Syst Man Cyb 1979; 9: 62–66. DOI: 10.1109/TSMC.1979.4310076

[13] Wagsta K, Cardie C, Rogers S, Schroedl S. .Constrained K-means Clustering with Background Knowledge. In: Proc. of the Eighteenth International Conference on Machine Learning (ICML 2001). 2001 ;1: 577-584.

[14] Dempster AP, Laird NM, Rubin DB. Maximum Likelihood from Incomplete Data via the EM Algorithm. J R Stat Soc 1977; 39: 1–38. DOI: 10.1111/j.2517-6161.1977.tb01600.x

[15] Wen Y, He L, Von Deneen KM, Lu Y. Brain tissue classification based on DTI using an improved Fuzzy C-means algorithm with spatial constraints. Magn Reson Imaging 2013; 31: 1623-1630. DOI: 10.1016/j.mri.2013.05.007

[16] Demirkaya O, Asyali MK, Sahoo PK. Image Processing with MATLAB: Application in Medicine and Biology. USA: CRC Press, 2009.

[17] Nguyen DMH, Vu HT, Ung HQ, Nguyen BT. 3D-brain segmentation using deep neural network and Gaussian mixture model. In Proc. IEEE Winter Conf. Appl. Comput. Vis. (WACV). 2017; 1: 815–824. DOI:10.1109/WACV.2017.96

[18] Huo Y, Xu Z, Xiong Y, Aboud K, Parvathaneni P, Bao S, Bermudez C, Resnick SM, Cutting LE, Landman BA. 3D whole brain segmentation using spatially localized atlas network tiles. NeuroImage 2019; 194: 105-119. DOI: 10.1016/j.neuroimage.2019.03.041

[19] Ramzan F, Khan MUG , Iqbal S, Saba T, Rehman A. Volumetric Segmentation of Brain Regions From MRI Scans Using 3D Convolutional Neural Networks. IEEE Access. 2020; 8:103697-103709. DOI:10.1109/ACCESS.2020.2998901

[20] Kong Y, Chen X, Wu J, Zhang P, Chen Y, Shu H. Automatic brain tissue segmentation based on graph filter. BMC Med Imaging. 2018; 18(1):9. DOI:10.1186/s12880-018-0252-x

[21] Kamarujjaman and Maitra M. 3D unsupervised modified spatial fuzzy c-means method for segmentation of 3D brain MR image. Pattern Anal Applic 2019; 22: 1561–1571. DOI:10.1007/s10044-019-00806-2

[22] Elaff I, El-Kemany A, Kholif M. Universal and stable medical image generation for tissue segmentation (The Unistable method). Turk J Electr Eng & Comp Sci 2017; 25: 1070-1081. DOI:10.3906/elk-1509-100.

[23] O'Donnell LJ, Westin CF. An Introduction to Diffusion Tensor Image Analysis. Neurosurgery Clinics of North America. 2011; 22(2):185-196. DOI: 10.1016/j.nec.2010.12.004

[24] Kingsley PB. Introduction to diffusion tensor imaging mathematics: Part I. Tensors, rotations, and eigenvectors. Concept Magn. Reson. 2006; 28:101–122. DOI: 10.1002/cmr.a.20048

[25] Basser PJ, Mattiello J, LeBihan D. MR Diffusion Tensor Spectroscopy and Imaging. Biophys J 1994; 66: 259-267. DOI: 10.1016/S0006-3495(94)80775-1

[26] Basser PJ, Pierpaoli C. Microstructural and Physiological Features of Tissues Elucidated by Quantitative-Diffusion-Tensor MRI. J Magn Reson 1996; 111: 209–219. DOI: 10.1006/jmrb.1996.0086

[27] Vilanova A, Zhang S, Kindlmann G, Laidlaw D. An Introduction to Visualization of Diffusion Tensor Imaging and Its Applications. In: Weickert, Joachim, Hagen, Hans. Visualization and Processing of Tensor Fields. Berlin Heidelberg: Springer, 2005. pp 121 – 153.

[28] Holtmannspotter M, Peters N, Opherk C, Martin D, Herzog J, Bruckmann H, Samann P, Gschwendtner A, Dichgans M. Diffusion Magnetic Resonance Histograms as a Surrogate Marker and Predictor of Disease Progression in CADASIL: A Two-Year Follow-Up Study. Stroke 2005; 36: 2559-2565. DOI: 10.1161/01.STR.0000189696.70989.a4.

[29] Seehaus A, Roebroeck A, Bastiani M, Fonseca L, Bratzke H, Lori N, Vilanova A, Goebel R, Galuske R. Histological validation of high-resolution DTI in human post mortem tissue. Front Neuroanat; 2015; 9:98. DOI: 10.3389/fnana.2015.00098

[30] Dyrby TB, Lundell H, Burke MW, Reislev NL, Paulson OB, Ptito M, Siebner HR. Interpolation of diffusion weighted imaging datasets. Neuroimage, 2014: 103:202–213. DOI: 10.1016/j.neuroimage.2014.09.005